論文 / 著書情報
Article / Book Information

Title	Comparison of the surface electronic structure of H-adsorbed ZnO surfaces: An angle-resolved photoelectron spectroscopy study
Authors	K. Ozawa,K. Mase
Citation	Physical review. B, Condensed matter and materials physics, Vol. 83, ,
発行日/Pub. date	2011, 3
公式URL/Journal URL	http://journals.aps.org/prb/
権利情報/Copyright	Copyright (c) 2011 American Physical Society

Comparison of the surface electronic structure of H-adsorbed ZnO surfaces: An angle-resolved photoelectron spectroscopy study

Kenichi Ozawa[1,*] and Kazuhiko Mase[2]

[1]*Department of Chemistry and Materials Science, Tokyo Institute of Technology, Ookayama, Meguro-ku, Tokyo 152-8551, Japan*

[2]*Institute of Materials Structure Science, High Energy Accelerator Research Organization (KEK), Tsukuba 305-0801, Japan*

(Dated:)

Synchrotron-radiation angle-resolved photoelectron spectroscopy has been utilized to study the interaction of atomic H with nonpolar ZnO($10\bar{1}0$) surface and polar ZnO($000\bar{1}$) and (0001) surfaces. H adsorption leads to the semiconductor-to-metal transition on the ZnO($10\bar{1}0$) and ($000\bar{1}$) surfaces. Metallization is a consequence of the formation of a single metallic band within the potential well between the surface/vacuum interface barrier and the edge of the conduction band, which is bent downwardly at the surface. The electrons confined in the potential well exhibit a free-electron-like behavior along the surface parallel, realizing two-dimensional electron gas system. For the H/ZnO(0001) system, on the other hand, no feature associated with the metallic band is observed. Higher reactivity of the ZnO(0001) surface towards H than the other two ZnO surfaces is responsible for the different behavior for the modification of the surface electronic structure by H adsorption.

I. INTRODUCTION

Zinc oxide (ZnO) is a metal oxide widely used as catalysts,[1] chemical sensors,[2] and a variety of electronic and photonic devices.[3] Moreover, owing to unique nanoscale structures that ZnO can take, i.e., nanorods, nanowires, nanoribbons, etc.,[4] novel applications of ZnO are expected. Therefore, intensive theoretical and experimental efforts have been devoted to clarify bulk and surface properties of ZnO as well as characteristics of nanostructured ZnO.[5] However, many fundamental aspects on the nature of ZnO have long been unanswered, and some of them are still under debate. The origin of the *n*-type conductivity of ZnO is one of the controversial issues. Among several candidates,[6,7] density functional theory (DFT) study by Van de Walle has suggested the important role of unintentionally doped atomic hydrogen (H) to form shallow donor states.[8] Several follow-up studies have supported this theoretical prediction.[9]

The donor character of H in ZnO has long been recognized by the fact that H doping enhances electric conductivity of ZnO.[10] Not only doped H but adsorbed H can act as a charge donor. Heiland and Kunstmann examined sheet conductance of two polar ZnO surfaces, i.e., the O-polar ZnO($000\bar{1}$) and Zn-polar ZnO(0001) surfaces, in their pioneering work[11] and found a clear conductivity change by adsorption of atomic H and O. H adsorption leads to an increased surface conductivity, whereas adsorbed O reduces it. These changes are well explained by donor and acceptor characters of H and O, respectively, and their adsorption leads to the variation of the charge density in the space-charge layer by alternating the direction of band bending.[11]. More, recently, Wöll and co-workers[9,12] have indicated on the basis of the high-resolution electron energy loss spectroscopy (HREELS) measurements that adsorption of H on the nonpolar ZnO($10\bar{1}0$) surface and the O-polar ZnO($000\bar{1}$) surface results in an increase in the charge densities at the surfaces, in accordance with the results by Heiland and Kunstmann. A DFT calculation has given two metallic bands on the H/ZnO($10\bar{1}0$) surface, on which the H atoms are bonded only to the surface O atoms.[12] On the basis of these results, the authors have concluded that the semiconductor-to-metal transition is induced on the ZnO surfaces by H adsorption.

An interesting point that the DFT study[12] has implicated is a significant lowering of the ZnO conduction band; the bottom of the conduction band minimum (CBM) reaches the top of the valence band maximum (VBM) at the center of the surface Brillouin zone (SBZ).[12] Namely, the gapless band structure is predicted. However, our angle-resolved photoelectron spectroscopy (ARPES) studies on H/ZnO($10\bar{1}0$)[13,14] reveals that the overall modification of the surface electronic structure is only slightly. The surface turns to be metallic with a single partially filled band at the center of the SBZ, while the band gap remains open. From these observation, we have proposed that the H-induced metallization of ZnO($10\bar{1}0$) proceeds via charge transfer from H to ZnO and the formation of the charge accumulation layer as a result of downward bending of the ZnO band at the surface.[13,14] Our result is the first direct evidence for the conventional view of the formation of the charge accumulation layer on the H/ZnO surfaces.[11] Nevertheless, H-induced modification of the electronic structures of the O-polar ZnO($000\bar{1}$) and Zn-polar ZnO(0001) surfaces is less known in comparison with the nonpolar surface, although the increased surface conductivity of both polar surfaces[11] and metallicity of the O-polar surface[9] have been implicated.

The interaction manner of H with the single-crystal ZnO surfaces is quite different depending on the surface orientation. Atomic force microscopy (AFM) and spectroscopic ellipsometry studies[15] have revealed that the Zn-polar (0001) surface is easy to be etched by atomic H, while the O-polar ($000\bar{1}$) surface is passivated upon the formation of the (1×1) H-covered surface. The reactivity of the non-polar ZnO($10\bar{1}0$) surface is between those of

ZnO(0001) and ZnO(000$\bar{1}$).[15] Difference in the bonding strength between O–H and Zn–H should be responsible for the different surface reactivity towards H[8].

In the present study, we have investigated the electronic structures of the H-covered polar and nonpolar ZnO surfaces by ARPES utilizing synchrotron radiation light and examined how the difference in the atomic structure and composition of the ZnO surfaces affects the H-induced changes in the surface electronic structure. It is found that H adsorption induces a single free-electron-like metallic band at the center of the SBZ on both ZnO(10$\bar{1}$0) and O-polar ZnO(000$\bar{1}$) surfaces. On the other hand, no evidence associated with surface metallicity is obtained on the Zn-polar ZnO(0001) surface. Magnitude of H-induced band bending and the surface roughness as a result of the etching by atomic H are crucial factors for metallicity of the H-covered ZnO surfaces.

II. EXPERIMENT

The ARPES measurements were performed at the beamline 11D of the Photon Factory, High Energy Accelerator Research Organization (KEK). The ultrahigh vacuum (UHV) analysis chamber with base pressure of 4 $\times$ 10^{-8} Pa was equipped with a hemispherical electron energy analyzer (Scienta SES 200) with a typical overall energy resolution of 50–70 meV at the photon energies ($h\nu$) between 60 and 70 eV. The spectra were acquired using the light linearly polarized within the incidence plane, while the incidence plane of the light was set parallel to the detection plane of the photoelectrons. The measurements were conducted at room temperature. The electron binding energy of the spectra presented in this paper is referenced to the Fermi energy (E_F), which was determined from the Fermi cut-off in the spectra of the Ta sample holder. Because of the semiconducting nature of ZnO, sample charging during photon irradiation was carefully checked by reducing the incident photon flux. The shift of the ARPES spectra by 0.1–0.3 eV towards the higher-binding-energy side was sometimes observed on the clean ZnO surfaces. No charging was encountered on the H-exposed surfaces. For the clean spectra presented below, the shift by surface charging, if existed, was corrected.

Single crystal ZnO samples with (10$\bar{1}$0) and (0001)/(000$\bar{1}$) orientation were purchased from SPC Goodwill, Russia. The sample crystals with $10 \times 10 \times 0.5$ mm^3 dimension were both-side polished. For the ZnO crystals with (0001)/(000$\bar{1}$) orientation, one side is the Zn-polar (0001) orientation and the other is the O-polar (000$\bar{1}$) orientation. The surface orientations were distinguished by the well-known difference in the surface etching behavior in acid solution.[16] The *in situ* sample preparations were carried out in a preparation chamber, which was connected to the analysis chamber but was pumped separately to the base pressure of $\sim$ 2 $\times$ 10^{-7} Pa. The clean surfaces were obtained by cycles of Ar^+ sputtering (2 kV) and annealing in UHV at 1050–1100 K followed by annealing in O_2 atmosphere (1.3 $\times$ 10^{-4} Pa). The ZnO surfaces after this procedure gave (1$\times$1) low energy electron diffraction (LEED) patterns. The work functions of the clean surfaces, determined from the photon energy and the spectral width between the Fermi level and the secondary electron cut-off, were 4.5 eV, 5.1 eV, and 4.0 eV for ZnO(10$\bar{1}$0), ZnO(000$\bar{1}$), and ZnO(0001), respectively. The work functions were in line with the trend expected from the surface atomic composition of ZnO.

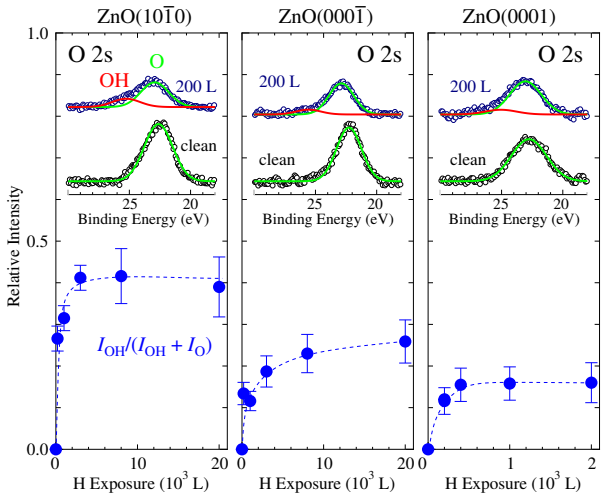

FIG. 1: Plots of relative intensities of the O 2s emission peaks from the OH component to the total O 2s peak intensities on ZnO(10$\bar{1}$0), ZnO(000$\bar{1}$) and ZnO(0001) against H exposure. The insets show O 2s core-level spectra ($h\nu$ = 65 eV) for the clean and 200-L H-dosed surfaces. The spectra were measured at the detection angle of 60° from the surface normal direction to enhance the surface sensitivity. The spectra shown here are those after subtracting polynomial background curves. The O 2s components are reproduced by Gaussian functions.

Hydrogen was adsorbed on the ZnO surfaces by backfilling the preparation chamber with H_2 (in the order of 10^{-4} Pa) while two tungsten filaments, placed at $\sim$ 15 cm away from the sample surfaces, were heated to 2100–2200 K to atomize H_2. The sample surfaces were kept at 300–350 K during H exposure. The efficiency of H_2 cracking was not estimated in the present study. However, a certain fraction of H_2 was atomized on the hot filaments because the sticking efficiency was appreciably increased in comparison with H_2 exposure without the hot filaments.

III. RESULTS

Adsorption of the H atoms on the ZnO surfaces gives a shifted component in the O 2s core-level region as shown in the inset figures in Fig. 1. The shifted component is associated with the OH species.[17,18] Plots of relative

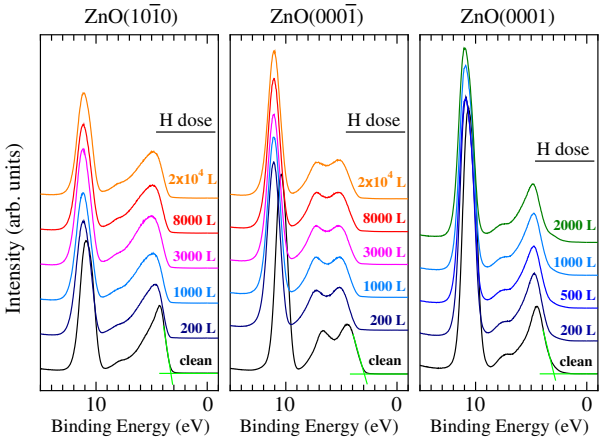

FIG. 2: Angle-integrated valence-band photoemission spectra of the ZnO(10$\bar{1}$0), (000$\bar{1}$) and (0001) surfaces exposed to various amounts of H. The photon energy used was 65 eV.

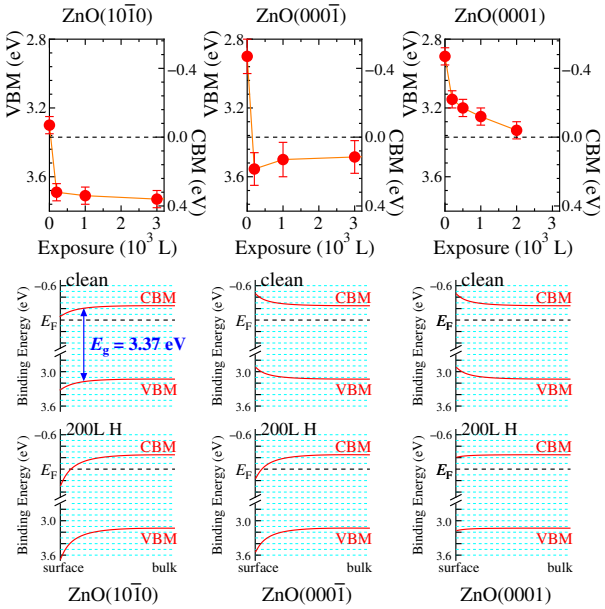

FIG. 3: (Upper) Changes of the VBM positions as a function of H exposure. The VBM positions are determined by extrapolating the leading edge of the valence-band emission to the baseline in the case of the clean surfaces, and the Zn 3d peak shifts are used to reproduce the H-induced shift of the VBM. Assuming the band-gap energy of ZnO (3.37 eV[5]), the CBM positions can be estimated from the VBM positions. The horizontal dotted line in each panel is drawn at 3.37 eV on the left axis and at 0.0 eV on the right axis. (Lower) Schematic of the energy band structures of the clean and 200-L H-dosed surfaces.

intensities of the OH components to the total O 2s intensities against H exposures, given in Langmuir units (1 L = 1.3 $\times$ 10^{-4} Pa s), are also shown in Fig. 1. The sticking probability of H is gradually lowered with increasing H exposures, and the relative intensities seem to reach saturation values on all surfaces. It is noted that some fraction of adsorbed H possibly diffuses into the bulk, owing to a relatively small diffusion barrier of H in ZnO.[19] Thus, the OH peak should include a contribution from the OH species in the subsurface region.

Figure 2 shows angle-integrated spectra of three low-index ZnO surfaces exposed to various amounts of H. The valence band of ZnO is composed of the O 2p-dominant O 2p–Zn 4sp hybridized band and the Zn 3d band.[20] For all three ZnO surfaces, the emission from the hybridized band is observed between 3 and 9 eV, and the Zn 3d emission is seen as an intense sharp peak at 10–11 eV. Different emission features depending on the surface termination is recognized in the O 2p–Zn 4sp band. In addition, the energy position of the valence band also depends on the surfaces; the valence bands of both O-polar and Zn-polar surfaces appear at shallower binding energies than that of ZnO(10$\bar{1}$0). The VBMs of the clean surfaces, determined by extrapolating the leading edge of the valence-band emission to the baseline, are 3.3 eV for ZnO(10$\bar{1}$0) and 2.9 eV for both polar ZnO surfaces. This means that the ZnO band bends slightly downwardly on ZnO(10$\bar{1}$0), while upward band bending is realized on the polar surfaces, because the bulk VBM is located at 3.1–3.2 eV below E_F.[21]

H adsorption on ZnO leads to the energy shift of the valence-band spectra towards a higher-binding-energy side (Fig. 2). The shift should originate from band bending because all the ZnO-related peaks (O 2s, Zn 3d, and Zn 3p peaks) show the same energy shift. Thus, adsorbed H acts as a charge donor and induces downward bending irrespective of the surface termination. Upper panels in Fig. 3 show the exposure dependence of the VBM positions. On ZnO(10$\bar{1}$0) and ZnO(000$\bar{1}$), the behavior of band bending is similar; a small exposure (200 L) is required to induce large downward bending [0.40 eV and 0.65 eV for ZnO(10$\bar{1}$0) and (000$\bar{1}$), respectively], and further exposures result in small changes. On the other hand, the band on ZnO(0001) bends gradually with increasing H exposure from 2.9 eV to 3.3 eV up to 2000 L. Schematics of the energy band structures of the clean and 200-L H-dosed surfaces are shown in the lower part of Fig. 3.

A donor character of adsorbed H on the ZnO surfaces can also be deduced by inspecting the H-induced change in the ionization energy (ΔI). ΔI is given by the sum of the magnitude of band bending ($e\Delta V_s$; $e\Delta V_s > 0$ for downward bending and $e\Delta V_s < 0$ for upward bending) and the work function change ($\Delta\Phi$),[22] and is a direct measure of the induced dipole moment (μ) through the Helmholtz equation;[23] $\mu = -2\epsilon_0\Delta I/\Theta_H$, where ϵ_0 is the permittivity constant and Θ_H is the H coverage.

Figure 4 shows the H-exposure dependence of ΔI, $e\Delta V_s$ and $\Delta\Phi$ for the three H/ZnO systems. $\Delta\Phi$ was estimated from the energy shift of the low kinetic-energy cut-off position of the secondary electron background, and $e\Delta V_s$ was deduced from the Zn 3d peak shift. Aside from the magnitude, the exposure dependence of the

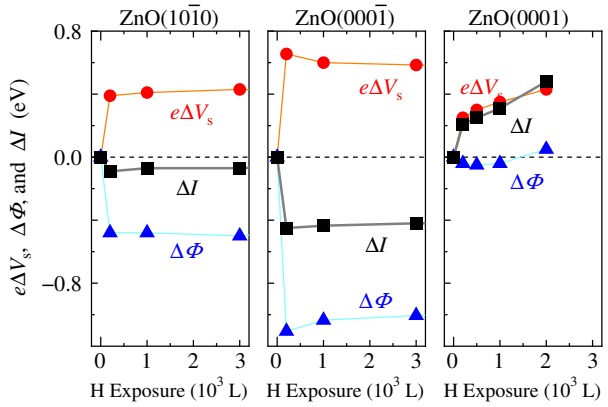

FIG. 4: Hydrogen exposure dependences of the magnitude of band bending ($e\Delta V_s$), the work function change ($\Delta\Phi$) and the change in the ionization energy (ΔI). $e\Delta V_s$ is positive (negative) for downward (upward) band bending. $\Delta I = e\Delta V_s + \Delta\Phi$.

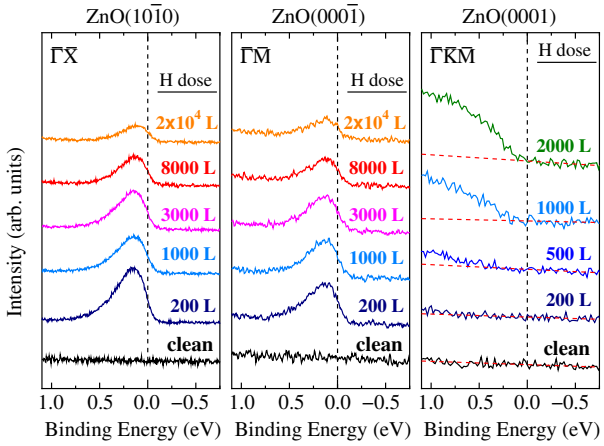

FIG. 5: Photoemission spectra in the vicinity of E_F of three ZnO surfaces at various H exposures. The photon energy was 65 eV. Each spectrum is constructed by integrating the ARPES spectra with detection angles between −4.5° and 4.5° along the high symmetry axes of the SBZ indicated in each panel. Dotted lines in the right panel are the backgrounds. Essentially the same sets of spectra are obtained when integrating along other high symmetry axes.

three parameters are similar for the H/ZnO(10$\bar{1}$0) and H/ZnO(000$\bar{1}$) systems; namely, a large change at the initial stage (200 L) followed by a gradual change at the higher exposures. ΔI is negative for these two systems, meaning the formation of the surface dipole moments with negative ends pointing towards the bulk inside. A larger negative value for H/ZnO(000$\bar{1}$) ($\Delta I = -0.4$ eV) than for ZnO(10$\bar{1}$0) (−0.1 eV) indicates that the larger dipole moment is formed on the O-polar ZnO surface. Although a fraction of adsorbed H on these surfaces should diffuse into the bulk, a majority of adsorbed H is considered to exist on the surfaces. Therefore, the cationized state of adsorbed H on ZnO(10$\bar{1}$0) and ZnO(000$\bar{1}$) is highly plausible.

A situation for the H/ZnO(0001) system is different from the other two systems. H adsorption affects the work function only slightly; $\Delta\Phi = -0.05$ eV at 200–1000 L, and +0.05 eV at 2000 L. On the other hand, $e\Delta V_s$ is sizable with positive values. Thus, the resultant ΔI values are positive, indicating the formation of the surface dipole moment with the negative end pointing towards the vacuum side. If adsorbed H on ZnO(0001) is cationized as expected from downward band bending ($e\Delta V_s > 0$), this result implies that the amount of subsurface H cations may surpass that of the H cations on top of the surface. Alternatively, the H-exposed ZnO(0001) surface could be so rough as a result of etching by atomic H[15] that the surface atomic and electronic structures are largely modified. In such a case, a donor character of adsorbed H cannot be determined only from the ΔI values. Nevertheless, downward band bending is suggestive of the donor character of adsorbed H on ZnO(0001).

Figure 4 clearly demonstrates that the H-induced changes of the surface electronic properties are similar for ZnO(10$\bar{1}$0) and ZnO(000$\bar{1}$), whereas the ZnO(0001) surface exhibits different response to H. Similarity and dissimilarity of the ZnO surfaces towards H are also recognized in the valence-band photoemission spectra. The spectra in Fig. 2 seem to bear no emission structures in the band gap region at first glance for all three systems. However, a close examination of the spectra reveals a density of states (DOS) at around E_F. Figure 5 shows the results of detailed measurements in the vicinity of E_F. The spectra are obtained by integrating the ARPES spectra with the emission angles between −4.5° and 4.5° (0° corresponds to the surface normal direction) along the selected high symmetry axes of the SBZ. For both ZnO(10$\bar{1}$0) and ZnO(000$\bar{1}$) surfaces, H adsorption induces the DOS with a skewed triangle shape at around E_F. Our previous ARPES studies have revealed that metallicity of the H/ZnO(10$\bar{1}$0) surface is accompanied by the formation of this characteristic DOS at E_F.[13,14] Thus, the ZnO(000$\bar{1}$) surface also turns to be metallic upon H adsorption. More straightforward evidence for surface metallization of the O-polar surface will be presented below. The emission intensities of the H-induced states are gradually diminished with increasing H exposure on both ZnO(10$\bar{1}$0) and ZnO(000$\bar{1}$), but surface metallicity is persistent up to relatively high exposures (at least up to 2×10^4 L).

Regarding the Zn-polar ZnO(0001) surface, the structure and the energy position of the H-induced states are completely different. The H-induced emission is first observed at 500 L in the energy region higher than 0.5 eV. The onset position of the DOS moves towards E_F with H exposure along with the increase in the emission intensity. However, no state is emerged at E_F even at 2000 L, indicating that the semiconducting nature of the ZnO(0001) surface is preserved after H adsorption.

In order further to clarify the metallic nature of the H-

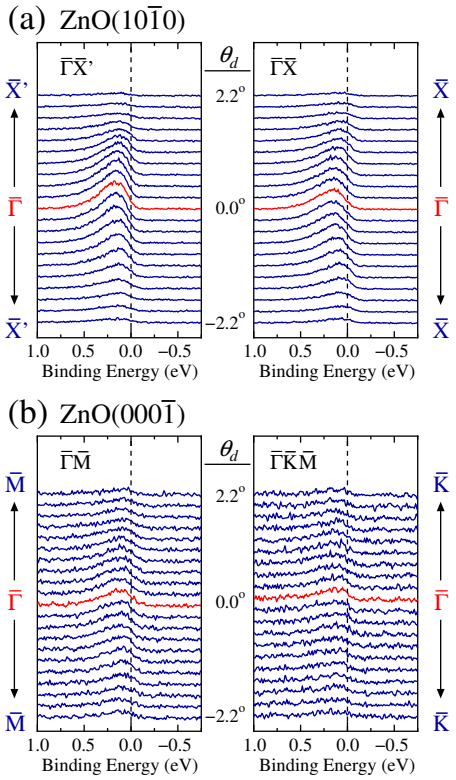

FIG. 6: Detection-angle-dependent spectra of the H-induced states of the 200-L H-exposed surfaces of ZnO(10$\bar{1}$0) and ZnO(000$\bar{1}$) along the high symmetry axes of the SBZ. The detection angle (θ_d) is measured from the surface normal direction. The photon energy used was 65 eV.

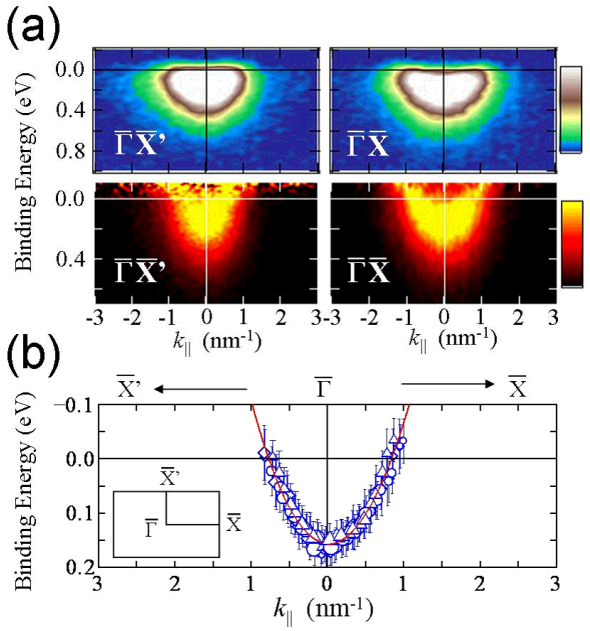

FIG. 7: (a) Plots of the raw emission intensity of the ARPES spectra (upper panels) and those divided by a GFD function (lower panels) along two high-symmetry axes for the 200-L H-dosed ZnO(10$\bar{1}$0) surface. The bright regions correspond to the high-emission-intensity regions. (b) Band structure of the H-induced state formed on ZnO(10$\bar{1}$0) by H exposure (200 L). The plotted points correspond to the peak positions in the GFD-function-divided ARPES spectra. The size of the symbols represents the emission intensity, and the different symbols are the results of independent measurements. A solid line is a least-square fitted result by a parabolic function.

adsorbed ZnO(10$\bar{1}$0) and (000$\bar{1}$) surfaces, the dispersion relations of the H-induced states have been examined. Figure 6 shows detection-angle-dependent spectra of the H-induced states on the 200-L H-exposed surfaces along high symmetry axes of the SBZ. The H-induced state is clear in a narrow emission region between $-2°$ and $2°$ with the highest intensity in the normal emission spectra. Although a dispersive feature of the H-induced state is not as clear for the H/ZnO(000$\bar{1}$) system as for the H/ZnO(10$\bar{1}$0) system because of a poor signal-to-noise ratio, the H-induced states for both systems exhibit a parabolic dispersion. The $h\nu$-dependent measurements reveal the lack of energy dispersion of the H-induced states along the surface perpendicular component of the wave number ($k_\perp$).[14] Therefore, the H-induced states are the localized states at the ZnO surfaces.

The parabolic feature of the H-induced states is more easily recognized in ARPES-intensity plots shown in Figs. 7a and 8a. Upper panels are the intensity plots of the raw ARPES spectra, and the lower panels are those of the ARPES spectra which are divided by Gaussian-convoluted Fermi-Dirac (GFD) functions so that the effect of the Fermi cut-off is removed. It is apparent that the H-induced states on both surfaces form bands with parabolic dispersion along the surface parallel component

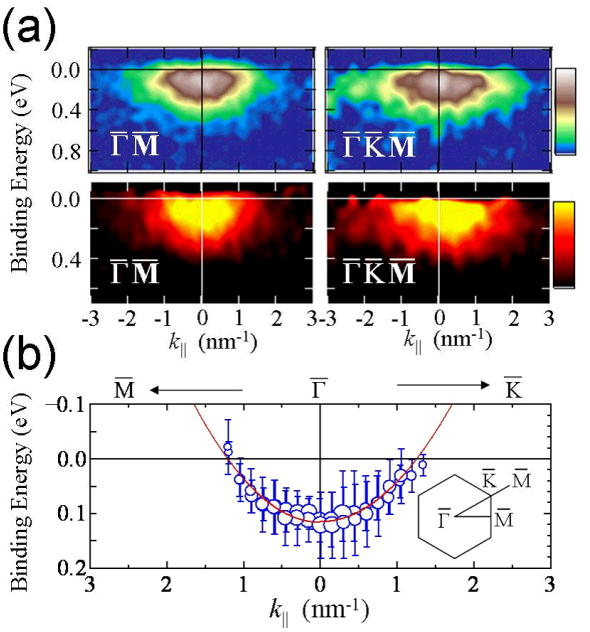

FIG. 8: Same as Fig. 7 but for the 200-L H-dosed ZnO(000$\bar{1}$) system.

of the wave number ($k_{\|}$).

Figure 7b shows the $k_{\|}$-dependence of the energy positions of the H-induced band for H/ZnO($10\bar{1}0$). The band has an isotropic structure on both $\overline{\Gamma X'}$ and $\overline{\Gamma X}$ axes and is reproduced well by parabola (solid line). The band is located at 0.16 ± 0.03 eV at $\overline{\Gamma}$ and disperses towards the shallower binding energies with increasing $k_{\|}$. The Fermi wave number ($k_{\rm F}$), where the band crosses $E_{\rm F}$, is 0.8 ± 0.1 nm^{-1}. For the H-induced states on ZnO($000\bar{1}$), the bottom of the band is 0.12 ± 0.06 eV at $\overline{\Gamma}$ and $k_{\rm F}$ is 1.2 ± 0.4 nm^{-1} on both $\overline{\Gamma M}$ and $\overline{\Gamma KM}$ axes. This is direct evidence for surface metallization of the O-polar ZnO($000\bar{1}$) surface.

No other state crossing $E_{\rm F}$ is found on both H/ZnO($10\bar{1}0$) and H/ZnO($000\bar{1}$) surfaces. Therefore, we conclude that metallicity of these surfaces is owing to the formation of the free-electron-like bands at around the $\overline{\Gamma}$ points.

IV. DISCUSSION

A. H/ZnO($10\bar{1}0$) and H/ZnO($000\bar{1}$)

In the present ARPES study, we have examined how the H-induced modification of the electronic structure depends on the differently terminated low-index surfaces of ZnO. A response to H adsorption is similar for the nonpolar ZnO($10\bar{1}0$) surface and the O-polar ZnO($000\bar{1}$) surface but is different for the Zn-polar ZnO(0001) surface (Figs. 3–5). For the Zn-polar surface, the semiconducting nature is preserved even when the surface is being covered with H. Contrastingly, the ZnO($10\bar{1}0$) and ZnO($000\bar{1}$) surfaces turn to be metallic. The origin of surface metallicity is the formation of a free-electron-like band in the vicinity of the center of the SBZ.

From the similarity of the surface electronic structures between H/ZnO($10\bar{1}0$) and H/ZnO($000\bar{1}$), the same metallization mechanism must be operative on these surfaces. Adsorbed H is cationized and induces downward band bending. The magnitude of band bending is sufficiently large so that the bottom of the conduction band, mainly composed of the Zn 4s orbitals, is shifted from above $E_{\rm F}$ to below $E_{\rm F}$. The upper panels in Fig. 3, showing the VBM positions, also indicate the CBM positions, which are determined from the VBM and the band-gap energy of 3.37 eV.[5] At 200-L H exposure, the CBMs are located at 0.32 eV and 0.18 eV below $E_{\rm F}$ on ZnO($10\bar{1}0$) and ZnO($000\bar{1}$), respectively. Since the CBM lies at 0.2–0.3 eV above $E_{\rm F}$ in the bulk,[21] the potential wells with the depths of ∼0.5 eV are created at these surfaces. Charge from adsorbed H should be, then, transferred to these potential wells and occupy the bands with parabolic energy dispersion along $k_{\|}$, reflecting the Zn 4s character of the conduction bands.

It should be pointed out that the depths of the surface potential wells could be even larger than ∼0.5 eV. A recent study by King et al. has demonstrated that the band gap of semiconducotor is diminished at the surface when the electron accumulation layer is formed.[24] The band-gap shrinkage is a consequence of the many-body interactions of the free carriers in the accumulation layer. In the present H/ZnO systems, the charge accumulation layers are also formed. Thus, the smaller band gap at the surface than in the bulk (3.37 eV) may be realized. In this case, the CBM positions are deeper than 0.32 eV and 0.18 eV on ZnO($10\bar{1}0$) and ZnO($000\bar{1}$), respectively, and thus the potential-well depths are larger than ∼0.5 eV.

In either cases, whether the surface band gap is diminished or not, the bottom positions of the metallic bands [0.16 eV and 0.12 eV for H/ZnO($10\bar{1}0$) and H/ZnO($000\bar{1}$) at 200 L, respectively] are shallower than the CBMs [≥ 0.32 eV and ≥ 0.18 eV]. It is highly probable that this discrepancy arises from the quantization of the metallic bands into discrete levels, and the bands observed in the present study should correspond to the lowest quantization levels. A lack of the energy dispersion of the H-induced states in $k_{\perp}$[14] and the parabolic dispersion in $k_{\|}$ indicate that the H-adsorbed ZnO($10\bar{1}0$) and ($000\bar{1}$) surfaces are viewed as two-dimensional electron gas (2DEG) systems.

Comparing the dispersion structure of the metallic bands (Figs. 7b and 8b), it is recognized that the curvature of the bands is different. Assuming the free-electron dispersion, the effective mass of the electrons ($m^*/m_{\rm e}$) is determined to be 0.16 ± 0.05 for H/ZnO($10\bar{1}0$). On the other hand, smaller curvature of the metallic band on H/ZnO($000\bar{1}$) gives a larger $m^*/m_{\rm e}$ value of 0.5±0.1. Different coordination of the Zn atoms on both ZnO surfaces may affect the spatial extent of the Zn 4s orbital and give the different band dispersion. However, more relevant explanation is that the distortion of the observed band by the Fermi cut-off is more significant on H/ZnO($000\bar{1}$) than on H/ZnO($10\bar{1}0$) because of a weaker emission intensity and a shallower positioning of the band (Figs. 6b and 8). Thus, the apparently high $m^*/m_{\rm e}$ value of 0.5 only indicates the upper limit.

The same may be said of the charge density of the 2DEG if the density is estimated from the band structure. Assuming the circular Fermi surfaces with the radii of $k_{\rm F}$ = 0.8±0.1 nm^{-1} and 1.2±0.3 nm^{-1} for H/ZnO($10\bar{1}0$) and H/ZnO($000\bar{1}$) at 200 L, respectively, the charge density is calculated to be $(1.0\pm0.2)\times10^{13}$ cm^{-2} for H/ZnO($10\bar{1}0$) and $(2.3\pm1.2)\times10^{13}$ cm^{-2} for H/ZnO($000\bar{1}$). Although the estimated value should provide the upper limit for the latter system, it is concluded that charge in the order of 10^{13} cm^{-2} is accumulated on the ZnO surfaces by H adsorption.

The estimated charge densities on the H/ZnO surfaces are in good agreement with the that of the 2DEG formed on ZnO($000\bar{1}$) recently reported by Piper et al. (2×10^{13} cm^{-2})[25] The authors have investigated the electronic structure of the O-polar ZnO($000\bar{1}$)-(1×1) surface and found the metallic band with a parabolic dispersion. Their reported band is nearly identical to that observed

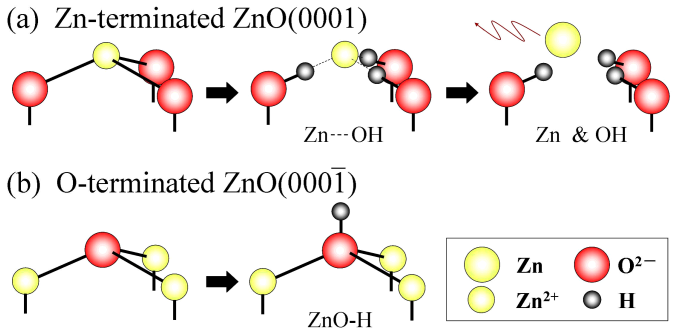

FIG. 9: Schematic of the reactions induced by H exposure on (a) Zn-polar ZnO(0001), and (b) O-polar ZnO(000$\bar{1}$), explaining the different etching behavior on these surfaces.

in the present study (Fig. 8). Interestingly, the O-polar ZnO surface Piper et al. examined was not treated by H. However, they have speculated that the surface is hydrogenated unintentionally by adsorption of gases in the UHV chamber, most probably water, so that the 2DEG was developed at the surface.[25] This suggests that only a small amount of H is required to develop the 2DEG on the ZnO surface. Actually, the drastic changes in band bending and the work function are induced up to 200 L on both ZnO(10$\bar{1}$0) and ZnO(000$\bar{1}$) (Fig. 4). Under the assumption, for simplicity in the calculations, that all adsorbed H atoms are on top of the ZnO surfaces and bulk diffusion is neglected, the H coverages $\Theta_{\rm H}$ at 200 L can roughly be estimated from the intensity ratio of the OH species (Fig. 1) to be 0.4 and 0.2 for H/ZnO(10$\bar{1}$0) and H/ZnO(000$\bar{1}$), respectively, where $\Theta_{\rm H} = 1.0$ corresponds to the O density on each ZnO surface [0.59×10^{15} cm^{-2} and 1.1×10^{15} cm^{-2} for ZnO(10$\bar{1}$0) and ZnO(000$\bar{1}$), respectively]. Thus, a large modification of the electronic structure is completed by a small amount of adsorbed H.

B. H/ZnO(0001)

Contrary to ZnO(10$\bar{1}$0) and ZnO(000$\bar{1}$), a metallic band is not formed on the Zn-polar ZnO(0001) surface. One reason is that H-induced band bending is so small that the CBM does not shift below $E_{\rm F}$ up to 2000 L (Fig. 3). This is not because the amount of adsorbed H on ZnO(0001) is small in comparison with the other two systems, as evident from Fig. 1. We consider that the roughness as a result of surface etching by atomic H should be the main reason for not only small band bending but also the peculiar H-exposure dependence of $\Delta\Phi$, $e\Delta V_{\rm s}$, and ΔI (Fig. 4).

AFM and spectroscopic ellipsometry studies by Bruno et al.[15] have revealed that ZnO(0001) is the most reactive surface among the low-index ZnO surfaces towards atomic H. The AFM image shows many clusters on ZnO(0001) after H exposure, and they are identified by X-ray photoelectron spectroscopy as Zn clusters.[15] Thus, significant reduction of ZnO (ZnO + H → OH + Zn) proceeds on ZnO(0001). The H-induced Zn clusters may be responsible for the band-gap state at > 0.5 eV at 500 L (Fig. 4). The onset position of this state moves from 0.5 eV to just below $E_{\rm F}$ at 2000 L. The shift should be induced along with the growth of the Zn clusters and be associated with an increasing efficiency of the final state screening towards photoholes after the photoemission process as the size of the cluster grows.[26–28] If the Zn clusters act as charge acceptor, a fraction of donated charge from H may reside on the clusters, not at the substrate surface. This can explain why the limited downward band bending is observed on the H/ZnO(0001) surface.

An easily-etched property of ZnO(0001) by atomic H may be partly explained by the local atomic structure on the surface. On the ideal surface, each surface Zn atom is bonded to three O atoms in the second layer. Since H atoms interact mainly with the O atoms at room temperature,[12] the H atoms should be inserted into the Zn–O backbonds to form three OH species and an isolated Zn atom to initiate surface etching. Contrastingly, the ZnO(000$\bar{1}$) surface is terminated by the O atoms, each of which is bonded to three Zn atoms. H atoms are bonded to the surface O atoms to give a stable H-terminated surface.[15] The situation on ZnO(10$\bar{1}$0) is in between two polar surfaces. Fig. 9 shows the reaction sequences on ZnO(0001) and ZnO(000$\bar{1}$).

The *real* ZnO surfaces are, however, not ideally terminated and, especially for the polar surfaces, several reconstructed structures have been reported; triangular-shaped reconstructions with (1×1) termination,[29–31] $(\sqrt{3}\times\sqrt{3})R30°$[32] and (1×3)[33] reconstructions on the Zn-polar surface, and the (1×3)[34], and $(\sqrt{3} \times \sqrt{3})R30°$[35] reconstructed surfaces on the O-polar surface. On the other hand, the polar ZnO surfaces we have prepared in the present study showed (1×1) LEED patterns, suggesting that the fraction of the reconstructed area, if exists, should be minor. Thus, the reaction model shown in Fig. 9 is still valid to a certain extent especially in the initial stage of the etching reaction. Atomic-level examination is required to fully understand the unique termination dependence of the etching behavior on the ZnO surfaces.

It is worth pointing out that, although the etching rate is much lower than that on ZnO(0001), the ZnO(10$\bar{1}$0) and (000$\bar{1}$) surfaces are also etched by H mainly from surface defect sites. As shown in Fig. 5, the emission intensities of the H-induced metallic states decrease with increasing H exposures. This change is associated with surface etching and resultant roughening of the surfaces. On the rough surfaces, $k_{\parallel}$ is no longer a good quantum number because of the loss of the translational symmetry. Furthermore, as in the case of the thin metal films in which discrete quantum-well states are formed,[36] it is important to prepare atomically uniform surfaces in order for the electrons confined in the potential well to fulfill the Bohr-Sommerfeld quantization condition; $2kt+\phi = 2n\pi$, where k is the perpendicular component of the electron

wave vector, t is the thickness of the potential well, ϕ is the total phase shift of reflection at the conduction band edge and the surface/vacuum interface, and n is a quantum number. For the system with the rough surface, the electrons are randomly reflected at the surface/vacuum interface so that the formation of the static standing wave within the potential well is suppressed. Therefore, even though the H atoms adsorb on the rough ZnO surfaces and induce downward band bending large enough that the lower part of the conduction band lies below $E_{\rm F}$, the metallic band should not be formed and the semiconductor-to-metal transition must be absent.

V. SUMMARY

The surface electronic structures of ZnO($10\bar{1}0$), ZnO($000\bar{1}$) and ZnO(0001) and their modification by adsorption of H have been examined by ARPES utilizing synchrotron radiation. H adsorption leads to the semiconductor-to-metal transition on the ZnO($10\bar{1}0$) and ZnO($000\bar{1}$) surfaces by forming single partially-filled metallic bands at the centers of the SBZs. Metallic charge behaves as a free-electron gas along the surface parallel, whereas it is confined in the potential wells between the conduction-band edge and the surface/vacuum interface so that the observed metallic bands should be quantized. On the other hand, no feature associated with surface metallization is found on the H/ZnO(0001) system. Although all of the ZnO surfaces are etched by atomic H, the etching rate is higher for ZnO(0001) than the other two surfaces, reflecting the difference in the surface atomic composition and structure. On the rough ZnO(0001) surface, the Zn clusters are formed and they should play a role to prevent surface metallization accompanied by H adsorption.

Acknowledgments

This work was supported by a Grant-in-Aid for Scientific Research (Grant No. 21560695) from Ministry of Education, Culture, Sports, Science, and Technology of Japan. The APRES measurements were performed under the approval of the Photon Factory Advisory Committee (Proposal No. 2008G016).

* Electronic address: ozawa.k.ab@m.titech.ac.jp

[1] K. C. Waugh, Catal. Today, **15**, 51 (1992).
[2] G. Errana, B. C. Joshi, D. P. Runthala, and R. P. Gupta, Crit. Rev. Solid State Mater. Sci. **29**, 111 (2004).
[3] D. C. Look, Mater. Sci. Eng. B **80**, 383 (2001).
[4] Z. L. Wang, Mater. Today, **7**, 26 (2004).
[5] Ü. Özgür, Ya. I. Alivov, C. Liu, A. Teke, M. A. Reshchikov, S. Doğan, V. Avrutin, S.-J. Cho, and H. Morkoç, J. Appl. Phys. **98**, 041301 (2005).
[6] D. C. Look, J. W. Hemsky, J. R. Sizelove, Phys. Rev. Lett. **82**, 2552 (1999).
[7] Y.-S. Kim and C. H. Park, Phys. Rev. Lett. **102**, 086403 (2009).
[8] C. G. Van de Walle, Phys. Rev. Lett. **85**, 1012 (2000).
[9] See, for example, H. Qiu, B. Meyer, Y. Wang, and C. Wöll, Phys. Rev. Lett. **101**, 236401 (2008).
[10] D. G. Thomas and J. J. Lander, J. Chem. Phys. **25**, 1136 (1956).
[11] G. Heiland and P. Kunstmann, Surf. Sci. **13**, 72 (1969).
[12] Y. Wang, B. Meyer, X. Yin, M. Kunat, D. Langenberg, F. Traeger, A. Birkner, and Ch. Wöll, Phys. Rev. Lett. **95**, 266104 (2005).
[13] K. Ozawa and K. Mase, Phys. Status Solidi A **207**, 277 (2010).
[14] K. Ozawa and K. Mase, Phys. Rev. B **81**, 205322 (2010).
[15] G. Bruno, M. M. Giangregorio, G. Malandrio, P. Capezzuto, I. L. Fragalà, and M. Losurdo, Adv. Mater. **21**, 1700 (2009).
[16] A. N. Marion and R. E. Hanneman, J. Appl. Phys. **34**, 384 (1963) .
[17] M. Kunat, St. Gil Girol, U. Burghaus, and Ch. Wöll, J. Phys. Chem. B **107**, 14350 (2003).
[18] J. Lahiri, S. Senanayake, and M. Batzill, Phys. Rev. B **78**, 155414 (2008).
[19] M. G. Wardle, J. P. Goss, and P. R. Briddon, Phys. Rev. Lett. **96**, 205504 (2006).
[20] W. Göpel, J. Pollmann, I. Ivanov, and B. Reihl, Phys. Rev. B **26**, 3144 (1982).
[21] The samples used in the present study have bulk carrier densities, determined by Hall-effect measurements, of 5×10^{13}–2×10^{15} cm^{-3} for ZnO($10\bar{1}0$) and $\sim10^{14}$ cm^{-3} for ZnO($000\bar{1}$) and ZnO(0001). From these values, the CBM position is calculated to be 0.2–0.3 eV above $E_{\rm F}$. Taking the band-gap energy of 3.37 eV into consideration, the VBM position in the bulk is estimated to be 3.1–3.2 eV below $E_{\rm F}$.
[22] P. Zurcher and R.S. Bauer, J. Vac. Sci. Technol. A 1, 695 (1983).
[23] C.T. Campbell, Surf. Sci. Rep. **27**, 1 (1997).
[24] P. D. C. King, T. D. Veal, C. F. McConville, J. Zúñiga-Pérez, V. Muñoz-Sanjosé, M. Hopkinson, E. D. L. Rienks, M. F. Jensen, and Ph. Hofmann, Phys. Rev. Lett. **104**, 256803 (2010).
[25] L. F. J. Piper, A. R. H. Preston, A. Fedorov, S. W. Cho, A. DeMasi, and K. E. Smith, Phys. Rev. B **81**, 233305 (2010).
[26] G. K. Wertheim, S. B. DiCenzo, and D. N. E. Buchanan, Phys. Rev. B **33**, 5384 (1986).
[27] H. Hövel, B. Grimm, M. Pollmann, and B. Reihl, Phys. Rev. Lett. **81**, 4608 (1998).
[28] K. Ozawa, T. Sato, Y. Oba, and K. Edamoto, J. Phys. Chem. C **111**, 4256 (2007).
[29] O. Dulub, L. A. Boatner, and U. Diebold, Surf. Sci. **519**, 201 (2002).
[30] O. Dulub, U. Diebold, and G. Kresse, Phys. Rev. Lett. **90**, 016102 (2003).
[31] F. Ostendorf, S. Torbrügge, and M. Reichling, Phys. Rev. B **77**, 041405(R) (2008).

[32] J. Dumont, B. Hackens, S. Faniel, P.-O. Mouthuy, R. Sporken, and S. Melinte, Appl. Phys. Lett. **95**, 132102 (2009).
[33] S. Torbrügge, F. Ostendorf, and M. Reichling, J. Phys. Chem. C **113**, 4909 (2009).
[34] M. Kunat, St. G. Girol, Th. Becker, U. Burghaus, and Ch. Wöll, Phys. Rev. B **66**, 081402(R) (2002).
[35] S. T. King, S. S. Parihar, K. Pardhan, H. T. Johnson-Steigelman, and P. F. Lyman, Surf. Sci. **602**, L131 (2008).
[36] T.-C. Chiang, Surf. Sci. Rep. **39**, 181 (2000).